Supporting Information

Table of Contents

1. Experimental Section

1.1 General

All reagents were purchased from commercial sources without further purification. Analytical reagent grade anhydrous dichloromethane (DCM) were directly used without further purification.

Compound **1**[1], **2**[2] were synthesized according to the reported procedure. ^{1}H and ^{13}C NMR spectra were recorded using Advance 600 MHz JEOL spectrometer and 2D ROESY spectra were recorded with JNM-ECZ600R/S1 spectrometer in $CDCl_3$, CD_2Cl_2, C_6D_6 with tetramethylsilane (TMS) as the internal standard. The chemical shift was recorded in ppm and the following abbreviations were used to explain the multiplicities: s = singlet, d = doublet, t = triplet, m = multiplet, br = broad. High-resolution (HR) APCI mass spectra were recorded on a ISQEM-ESI-APCI instrument, UV-vis absorption was recorded on a Shimadzu UV-3600 spectrophotometer. Cyclic voltammetry and differential pulse voltammetry measurements were performed in dry DCM on a DH7000C electrochemical analyzer with a three-electrode cell, using 0.1 M Bu_4NPF_6 as supporting electrolyte, AgCl/Ag as reference electrode, glassy carbon as working electrode, and Pt wire as counter electrode. The potential was externally calibrated against the ferrocene/ferrocenium couple. Single crystals were measured at low temperature (T = 113 K) on a four circles goniometer Kappa geometry Bruker AXS D8 Venture equipped with a Photon 100 CMOS active pixel sensor detector using a Copper monochromatized (λ = 1.54178 Å) X-Ray radiation.

Continuous wave X-band ESR spectra were obtained with a Bruker (EMX plus) spectrometer using a variable temperature liquid nitrogen cryostat. The VT ESR data of **CBQCz^{4+}(SbF$_6^-$)$_4$** in frozen state upon cooling from 200 K to 160 K were fitted by Bleaney-Bowers equation,

$$IT = \frac{C}{k_B[3 + exp(-2J/k_BT)]}$$

where C is a constant and -2J is correlated to the excitation energy from the singlet ground state to the triplet excited state.

1.2 Synthetic procedures and characterization data

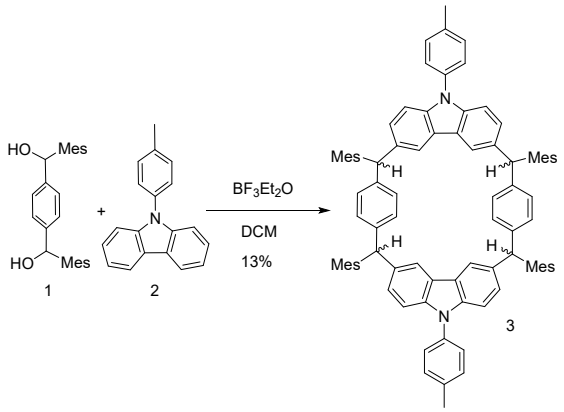

Under nitrogen atmosphere, compound **1** (257 mg, 1.0 mmol), compound **2** (374 mg, 1.0 mmol), BF_3Et_2O (300 μL, 2.2 mmol) were dissolved in dry DCM (370 ml). The reaction mixture was stirred for 20hrs at rt. Than the reaction was quenched with trimethylamine. The solvent was removed by rotary evaporation. The crude product was purified by a flash column chromatography on silica gel with petroleum ether/ DCM (1/2) as eluent to give the compound **3** (79 mg, 13% yield). ^{1}H NMR (600 MHz, $CDCl_3$) δ 7.96 (d, *J* = 14.5 Hz, 2H), 7.76-7.58(m, 2H)7.42 (q, *J* = 6.4 Hz, 4H), 7.37 – 7.31 (m, 4H), 7.27 (dd, *J* = 8.6, 4.5 Hz, 2H), 7.23 – 7.19 (m, 2H), 7.13 (dd, *J* = 16.5, 8.3 Hz, 6H), 7.08 – 6.98 (m, 2H), 6.96 – 6.84 (m, 8H), 6.79 – 6.73 (m,4H), 6.28 – 6.23 (m, 2H), 6.14 – 6.07 (m, 2H), 2.48 – 2.21 (m, 24H), 1.56 (s, 18H). ^{13}C NMR (125 MHz, $CDCl_3$) δ 140.66, 138.68, 138.17, 137.45, 136.62, 134.68, 132.56, 132.27, 130.47, 128.32, 128.23, 127.75, 126.61, 123.15, 122.76, 110.16, 32.03, 29.80, 29.47, 27.01, 22.80, 21.17, 20.48, 14.23. HRMS analysis (ACPI): calcd for $C_{90}H_{83}N_2$ $(M+H)^+$: 1191.65, found:1191.65564 (error: 4.7 ppm).

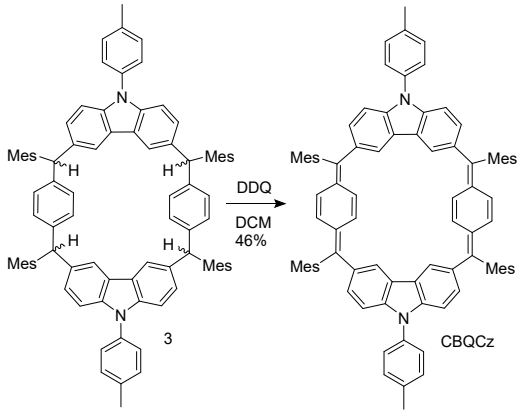

Under nitrogen atmosphere, compound **3** (60 mg, 0.005 mmol), DDQ (50 mg, 0.22 mmol) were dissolved in dry toluene (15 ml). The reaction mixture was stirred for 24hrs at rt. The solution was washed with brine and dried over anhydrous sodium sulfate. The solvent was removed and the residue was purified by column chromatography on silica gel with hexane/DCM (2/1) as eluent to give **CBQCz** (25 mg, 46% yield) ^{1}H NMR (600 MHz, C_6D_6) δ 9.33 (s, 4H), 8.12 (s, 4H), 7.06 (s, 13H), 6.96 (s, 4H), 6.90 (d, *J* = 8.3

Hz, 4H), 6.80 (s, 4H), 6.36 (d, J = 1.7 Hz, 4H), 2.38 (s, 12H), 2.22 (s, 13H), 2.13 (s, 12H), 2.05 (s, 6H). ^{13}C NMR (125 MHz, $CDCl_3$) δ 141.39, 141.26, 139.66, 137.98, 137.95, 137.76, 137.29, 135.96, 135.27, 134.28, 134.04, 130.54, 130.32, 129.36, 129.33, 127.82, 127.79, 126.96, 125.83, 123.38, 123.27, 120.83, 120.43, 119.71, 109.89, 109.58, 22.36, 21.37, 21.00. HRMS analysis (ACPI): calcd for $C_{90}H_{79}N_2$ $(M+H)^+$: 1187.62, found:1187.62299 (error: 2.5 ppm).

1.3 Chemical oxidation

CBQCz^{4+}(SbF$_6^-$)$_4$ were prepared by mixing **CBQCz** (19 mg, 0.01 mmol) and $AgSbF_6$ (15 mg, 0.044 mmol, 4.4 equiv.) together in dry DCM (5 mL). After 10 mins, the solution was subjected through a PTFE filter to remove the Ag powder. After evaporation of the solvent, the final product was obtained without further purification. The ESR spectrum was shown in Figure S4.

2. Dynamic NMR data analysis

Variable-temperature (VT) ^{1}H NMR spectra of **CBQCz** and **CBQCz^{4+}(SbF$_6^-$)$_4$** were recorded in C_6D_6 and CD_2Cl_2, respectively. The exchange rate constant k was estimated according to the literature.[3] Three characteristic exchange regions were observed in all cases if available: (1) a slow exchange region, in which the exchange is slower than the spectrometer timescale and two separate peaks are observed; (2) coalescence temperature, at which two peaks completely merge into one peak; and (3) fast exchange region, in which the exchange is rapid than the spectrometer and the two peaks are merged into one peak.

The exchange rate constant k was calculated by individual equation in these three regions.

(1) At slow exchange temperature ($T < T_c$), two peaks are separated obviously, then $k = \pi[(\Delta V_e)_{1/2}-(\Delta V_0)_{1/2}]$. When temperature is close to Tc, two separated peaks will overlap with each other but not be fully coalescent, and then equation $k = \pi[\Delta V_0^2-\Delta V_e^2]^{1/2}/2^{1/2}$ was used;

(2) At coalescence temperature ($T = T_c$), $k = \pi\Delta V_0/2^{1/2}$;

(3) At fast exchange temperature ($T > T_c$), $k = \pi\Delta V_0^2/2[(\Delta V_{e)1/2}-(\Delta V_0)_{1/2}]$.

In these equations, ΔV is the difference in chemical shift (Hz) between two correlated peaks at one temperature in the slow exchange region. ΔV_0 is defined as the value of ΔV at no exchange temperature (at which the two peaks are mostly separated), and ΔV_e is defined as the value of ΔV at all other temperatures in this region if available. $(\Delta V)_{1/2}$ is the linewidth (Hz) at half height of peak at any temperature in all region if available. $(\Delta V_0)^{1/2}$ is defined as the value of $(\Delta V)_{1/2}$ at no exchange temperature. $(\Delta V_e)_{1/2}$ is defined as the value of $(\Delta V)_{1/2}$ at all other temperatures in all region if available. Tc is defined as coalescence temperature at which two peaks completely merge into one peak.

The obtained k values were then fitted with Eyring equation: $\ln(k/T) = - \Delta H^{\ddagger}/R \bullet 1/T + \ln(k_B/h) + \Delta S^{\ddagger}/R$ to get the thermodynamic parameters $\Delta H^{\ddagger}$ and $\Delta S^{\ddagger}$, and then $\Delta G^{\ddagger} = \Delta H^{\ddagger} - T\Delta S^{\ddagger}$ (Table S1, Figure S1, Table S2, Figure S2).

Table S1. Parameters obtained from the line-shape analysis based on the VT ^{1}H NMR spectra of **CBQCz** in C_6D_6.

Temperature (K)	$(\Delta V_e)_{1/2}$ (Hz)	ΔV_e (Hz)	k (s^{-1})
298	**10.38** $(\Delta V_0)_{1/2}$	**110.88** (ΔV_0)	--
283	12.24	109.62	5.84
288	15.96	107.10	17.53
293	20.70	105.48	32.42
298	33.54	99.36	72.76
303	68.58	85.68	156.37
308	--	--	--
313 (T_c)	--	--	246.35
318	--	--	--
323	33.84	--	823.19
328	25.62	--	1267.19
333	18.96	--	2250.81
338	14.58	--	4598.09

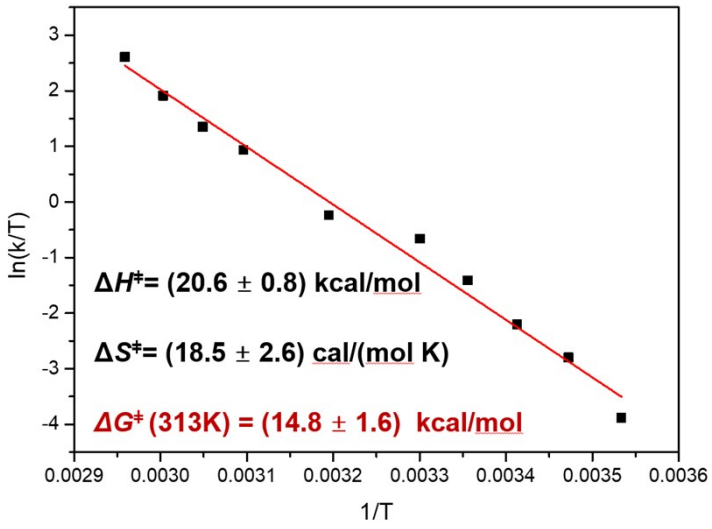

Figure S1. Fitting of the exchange rate constants with temperature by Erying equation for **CBQCz** in C_6D_6.

Table S2. Parameters obtained from the line-shape analysis based on the VT ^{1}H NMR spectra of **CBQCz^{4+}(SbF$_6^-$)$_4$** in CD_2Cl_2.

Temperature (K)	$(\Delta V_e)_{1/2}$ (Hz)	ΔV_e (Hz)	k (s^{-1})
183	**14.75** $(\Delta V_0)_{1/2}$	**109.35** (ΔV_0)	--
188	16.185	106.12	**58.6**
193	17.56	103.39	79.1
198	18.99	95.19	119.55
203	14.115	82.9	158.41
208 (T_c)	60.023		242.85
213	58.985	--	424.18
218	48.465	--	556.36
223	44.325	--	634.12
228	38.335	--	794.87

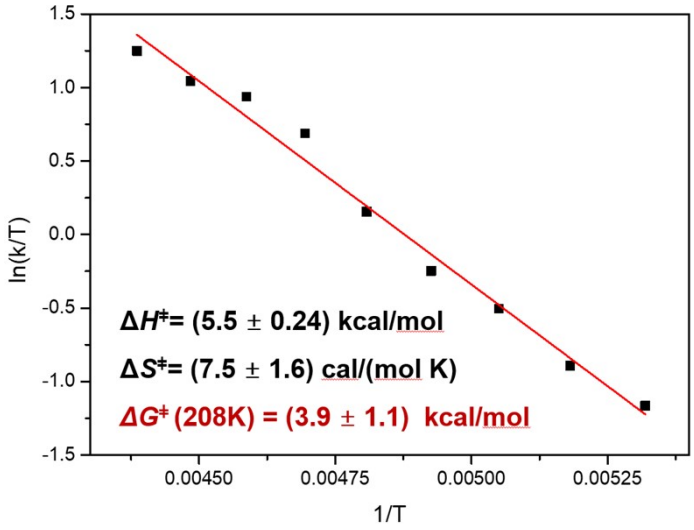

Figure S2. Fitting of the exchange rate constants with temperature by Erying equation for **CBQCz^{4+}(SbF$_6^-$)$_4$** in CD_2Cl_2.

3.Additional Spectra

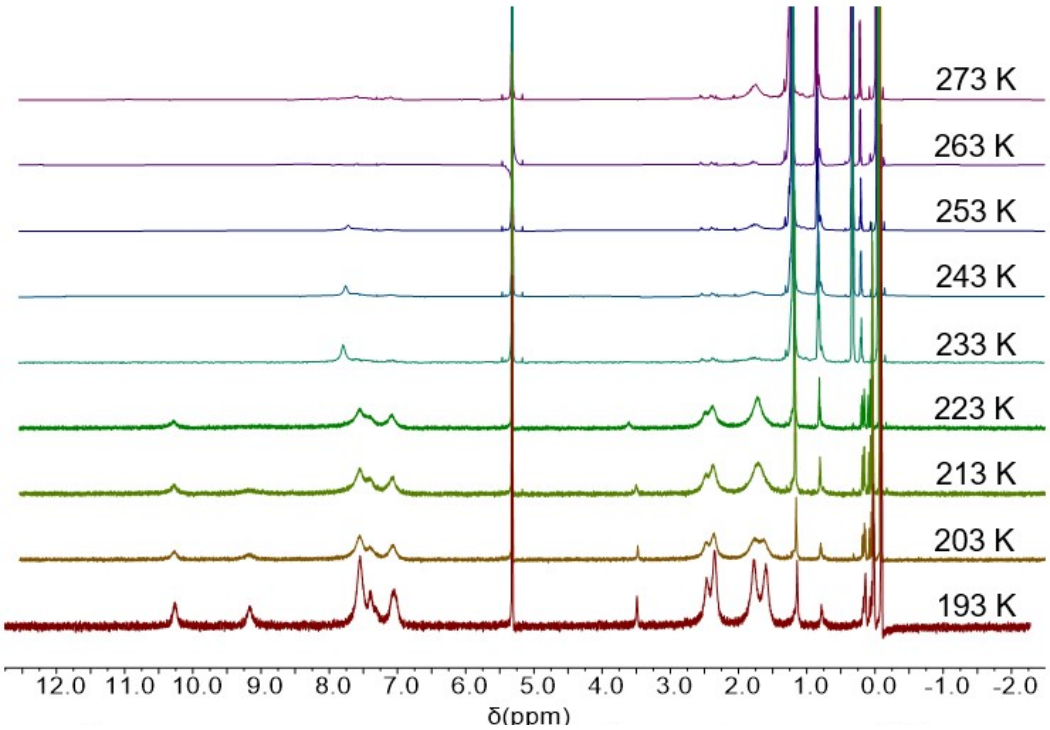

Figure S3. VT ^{1}H NMR spectra of **CBQCz^{4+}(SbF$_6^-$)$_4$** in CD_2Cl_2 solution from 193 K to 273 K.

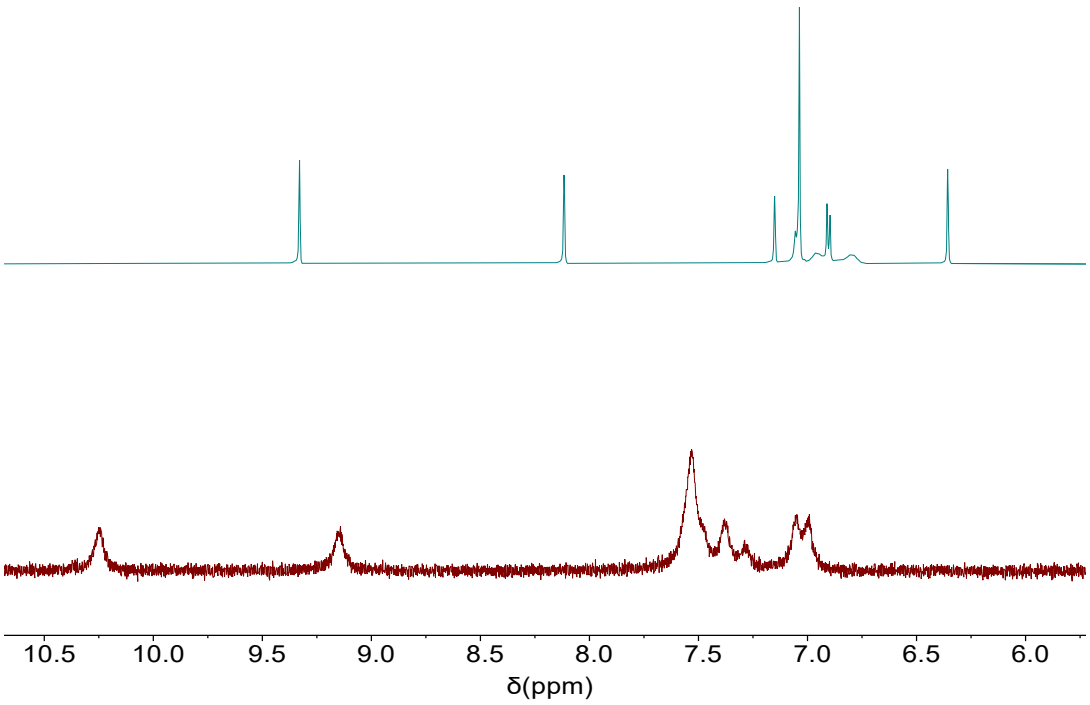

Figure S4. ^{1}H NMR spectra (aromatic region) of **CBQCz** (top) in C_6D_6 and **CBQCz^{4+}(SbF$_6^-$)$_4$** (bottom) in CD_2Cl_2.

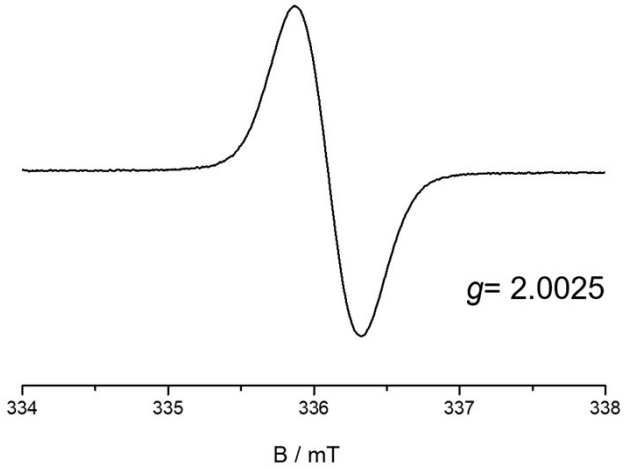

Figure S5. ESR spectra of **CBQCz^{4+}(SbF$_6^-$)$_4$**, recorded in DCM solution at room temperature, the cations were generated by oxidation of **CBQCz** with four equivalent of $AgSbF_6$.

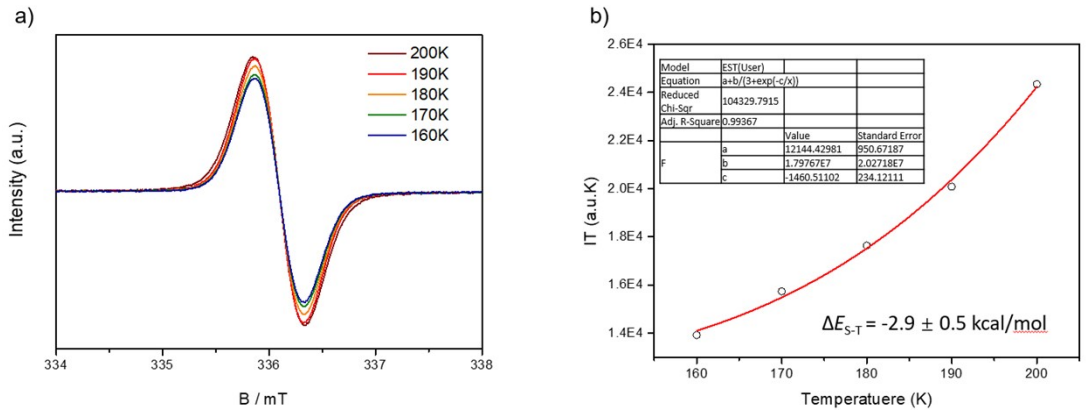

Figure S6. (a) VT ESR spectra of **CBQCz^{4+}(SbF$_6^-$)$_4$** recorded in the powder state (b) The product of ESR signal intensity (*I*) and temperature (*T*) *versus* temperature of **CBQCz^{4+}(SbF$_6^-$)$_4$** from 200 K to 160 K (black hollow dots) and the fitted curve by Bleaney–Bowers equation (red line).

Table S3. Electrochemical and optical data of **CBQCz**

Com.	λ_{max} (nm)	ε_{max} ($M^{-1}cm^{-1}$)	$E_{1/2}^{ox}$ (V)	HOMO (eV)	E^{opt} (eV)
CBQCz	418	9 x 10^5	-0.03, 0.00, 0.28, 0.57	4.77	2.72

$E_{1/2}^{ox}$ are the half-wave potentials for respective oxidation waves with Fc^+/Fc as reference. Electrochemical HOMO. were calculated from the onset values of oxidation and reduction potentials. λ_{abs}: main absorption peak. ε_{max}: molar extinction coefficient at the absorption maximum. E_g^{opt}: optical energy gap calculated from onset of the absorption maximum.

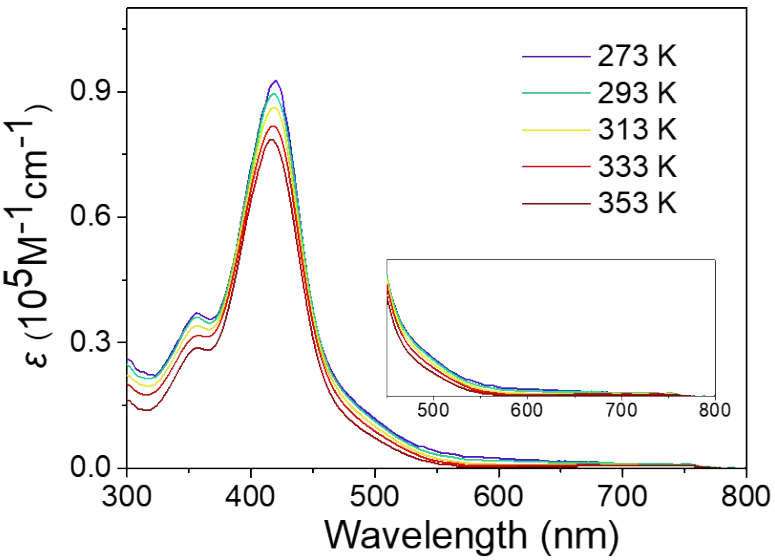

Figure S7. VT UV/Vis-NIR absorption spectra of neutral **CBQCz** in toluene from 353 K to 273 K.

4. Theoretical calculations

Density functional theory calculations were employed with Gaussian 09 package,[4] utilizing the B3LYP[5-8] level of theory with Pople basis set 6-31G(d,p)[7-9] for **CBQCz** in gas phase**,** and LC-UBLYP[10] level of theory with Pople basis set 6-31G(d,p) for **CBQCz**$^{4+}$ to estimate their open-shell characters with PCM model as solvation of dichloromethane.

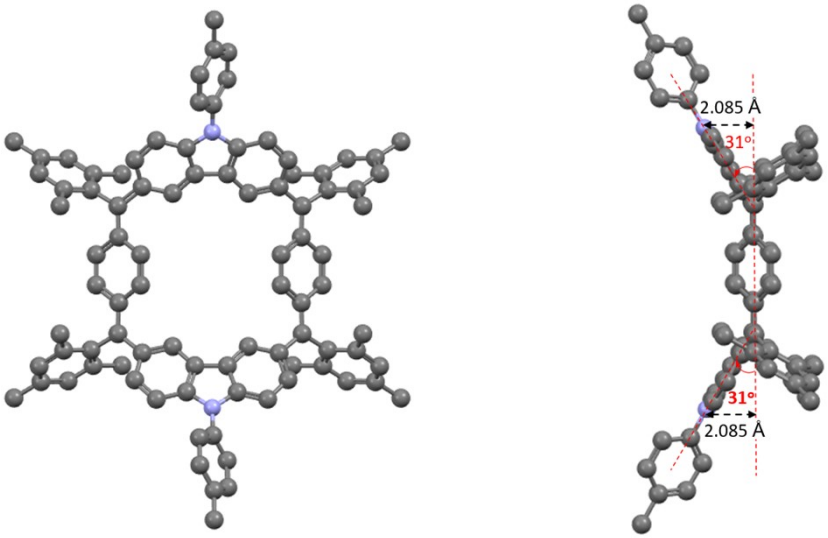

Figure S8. Optimized (B3LYP/6-31G(d,p)) structure of **CBQCz**.

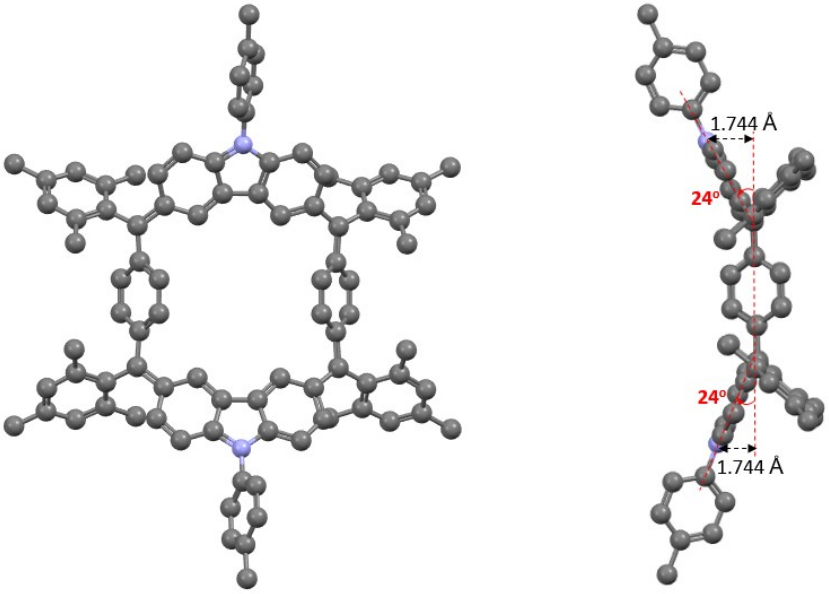

Figure S9. Optimized (LC-UBLYP/6-31G(d,p)) structure of **CBQCz**$^{4+}$ with PCM model as solvation of dichloromethane.

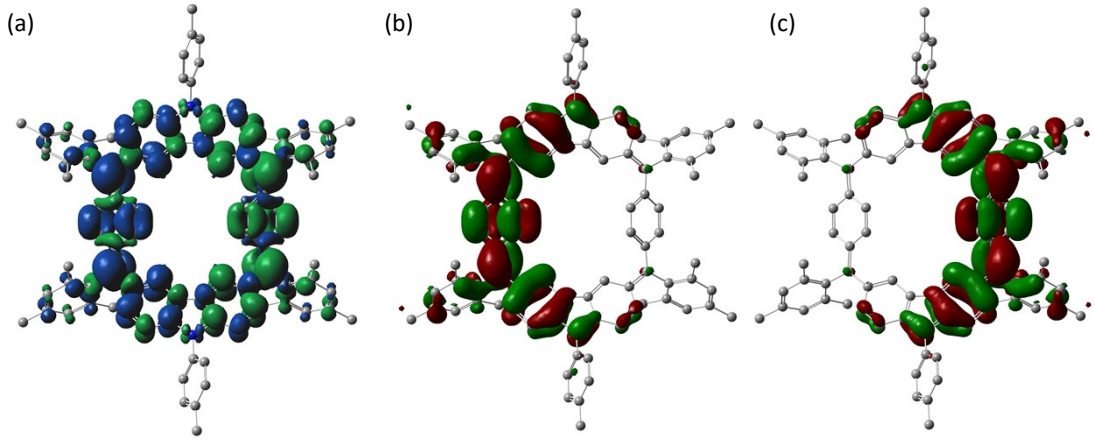

Figure S10. a) Calculated (UB3LYP/6-31G(d,p)) spin density distributions of **CBQCz**$^{4+}$, (b) Calculated (UB3LYP/6-31G(d, p)) HOMO α and HOMO β of **CBQCz**$^{4+}$.

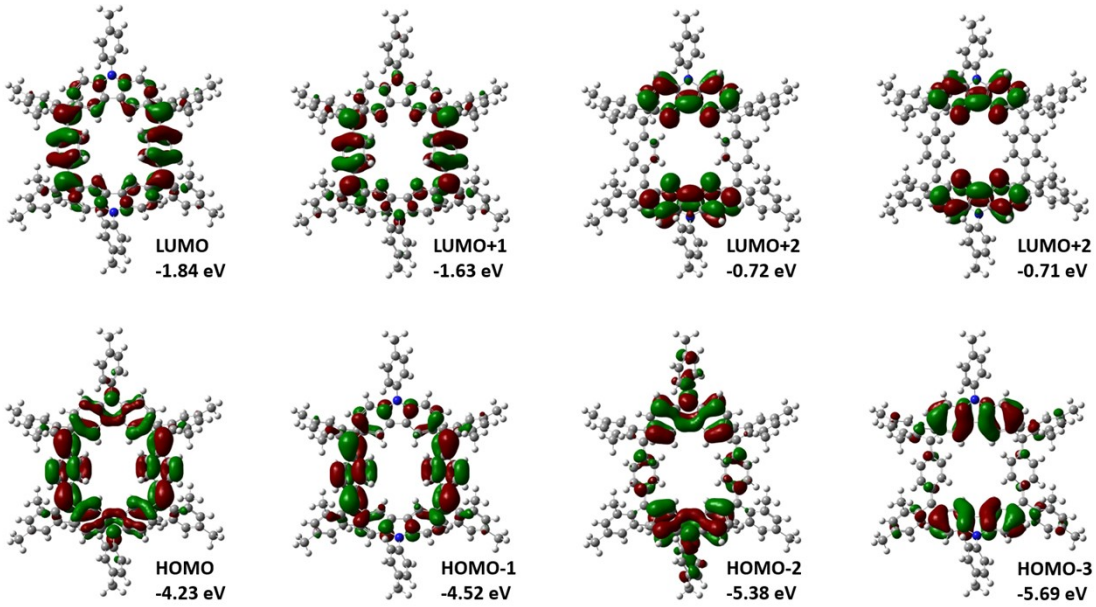

Figure S11. Frontier molecular orbital profiles and energy levels of **CBQCz** at the B3LYP/6-31G(d, p) level of theory.

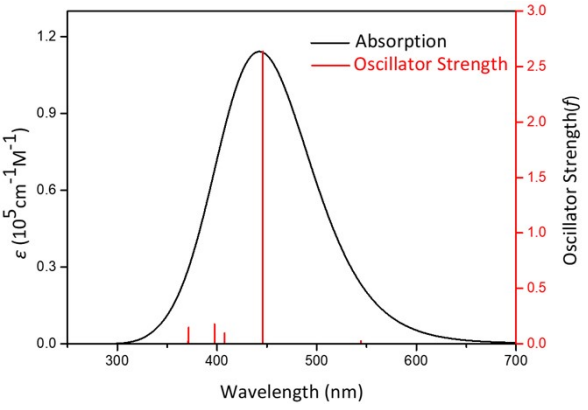

Figure S12. DFT calculated (B3LYP/6-31G(d, p)) absorption (black), fluorescence (red) spectra and their oscillator strengths of **CBQCz**.

Table S4. Selected TD-DFT (RB3LYP/6-31G(d,p)) calculated energy, wavelength, oscillator strength and compositions of major electronic transitions to the excited state of **CBQCz**

No.	Energy (eV)	Wavelength (nm)	Osc. Strength	Major contribs
1	2.0069	617.79	0.0	HOMO→LUMO (98%)
2	2.2788	544.08	0.0273	H-1->LUMO (41%), HOMO->L+1 (59%)
3	2.6082	475.36	0.0	H-1->L+1 (96%)
4	2.7820	445.67	2.6361	H-1->LUMO (57%), HOMO->L+1 (39%)
5	3.0449	407.19	0.0979	HOMO->L+2 (96%)
6	3.0526	406.16	0.0008	HOMO->L+3 (94%)
7	3.1210	397.26	0.1768	H-2->LUMO (92%)
8	3.3170	373.78	0.0	H-1->L+2 (92%)
9	3.3396	371.25	0.1467	H-1->L+3 (91%)
10	3.3448	370.68	0.0207	H-2->L+1 (91%)

5. Crystallographic data

Single crystals of **CBQCz** was obtained by dry hexane into their dichloromethane solutions.

Table S5. Crystallographic data for **CBQCz**.

Empirical formula	$C_{90}H_{78}N_2$	
Formula weight	1186.62	
Temperature	113(2) K	
Wavelength	0.71073 Å	
Crystal system	Triclinic	
Space group	P-1	
Unit cell dimensions	a = 12.2461(5) Å	α= 82.377(4)°.
	b = 17.5780(8) Å	β= 88.409(3)°.
	c = 17.8214(7) Å	γ= 74.137(4)°.
Volume	3657.4(3) Å^3	
Z	2	
Density (calculated)	1.078 Mg/m^3	
Absorption coefficient	0.061 mm^{-1}	
F(000)	1264.0	
Crystal size	0.22 x 0.20 x 0.17 mm^3	
Theta range for data collection	5.000 to 26.372°.	
Index ranges	-15<=h<=15, -21<=k<=21, -22<=l<=22	
Reflections collected	172951	
Independent reflections	55808 [R(int) = 0.1313]	
Completeness to theta = 25.027°	99.9 %	
Absorption correction	multi-scan	
Max. and min. transmission	0.000 and 0	
Refinement method	Full-matrix least-squares on F^2	
Data / restraints / parameters	14946 / 0 / 884	
Goodness-of-fit on F^2	1.003	
Final R indices [I>2sigma(I)]	R1 = 0.0720, wR2 = 0.2068	
R indices (all data)	R1 = 0.1335, wR2 = 0.3006	
Largest diff. peak and hole	0.58 and -0.21 e.Å^{-3}	

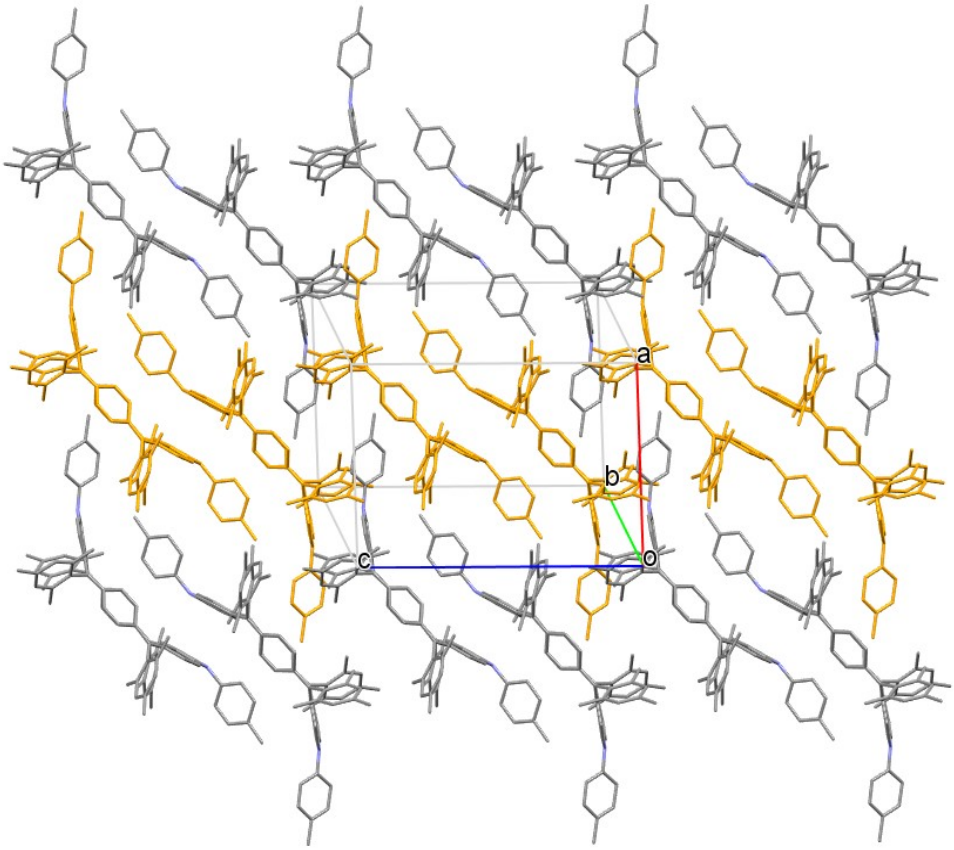

Figure S13. Molecular packing of **CBQCz**. All hydrogen atoms are omitted for clarity.

6. Appendix: NMR and APCI mass spectra of all new compounds

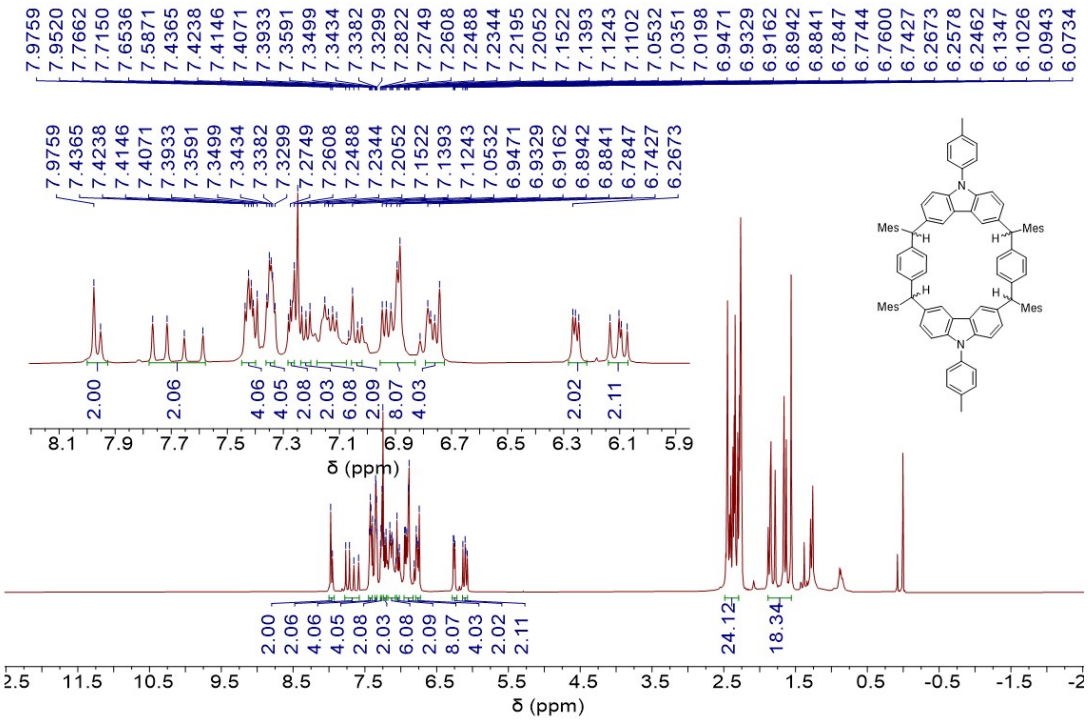

Figure S14. ^{1}H NMR spectrum of **3** (600 MHz, $CDCl_3$)

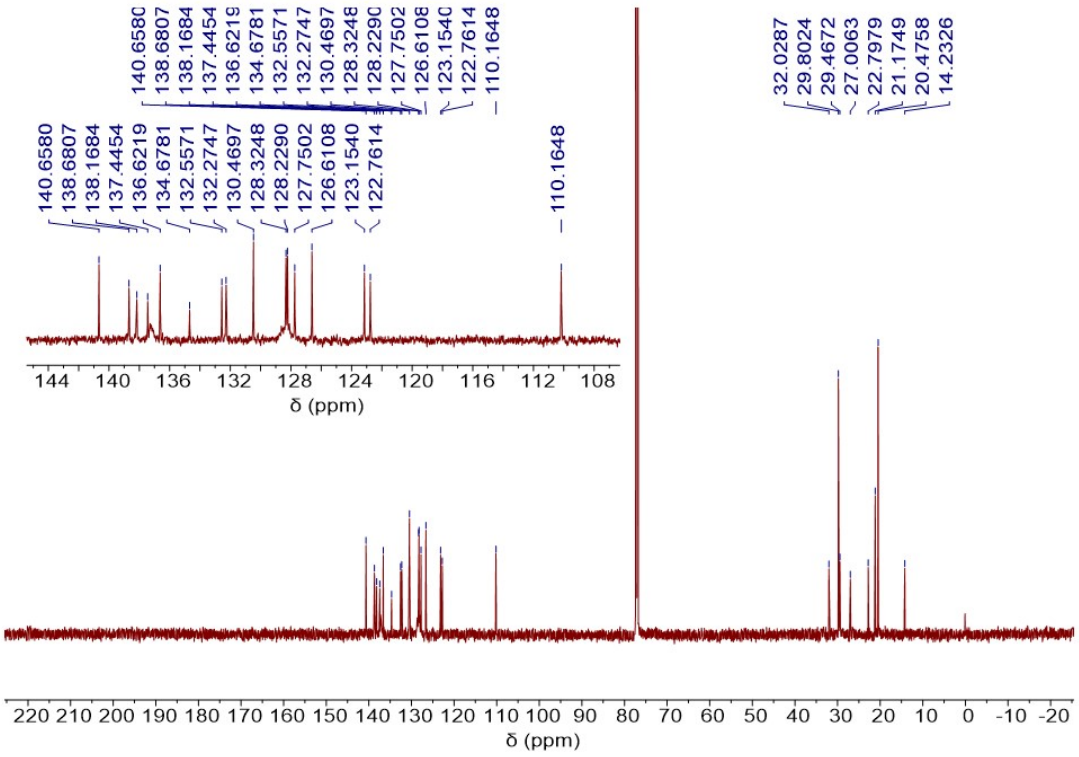

Figure S15. ^{13}C NMR spectrum of **3** (125 MHz, $CDCl_3$).

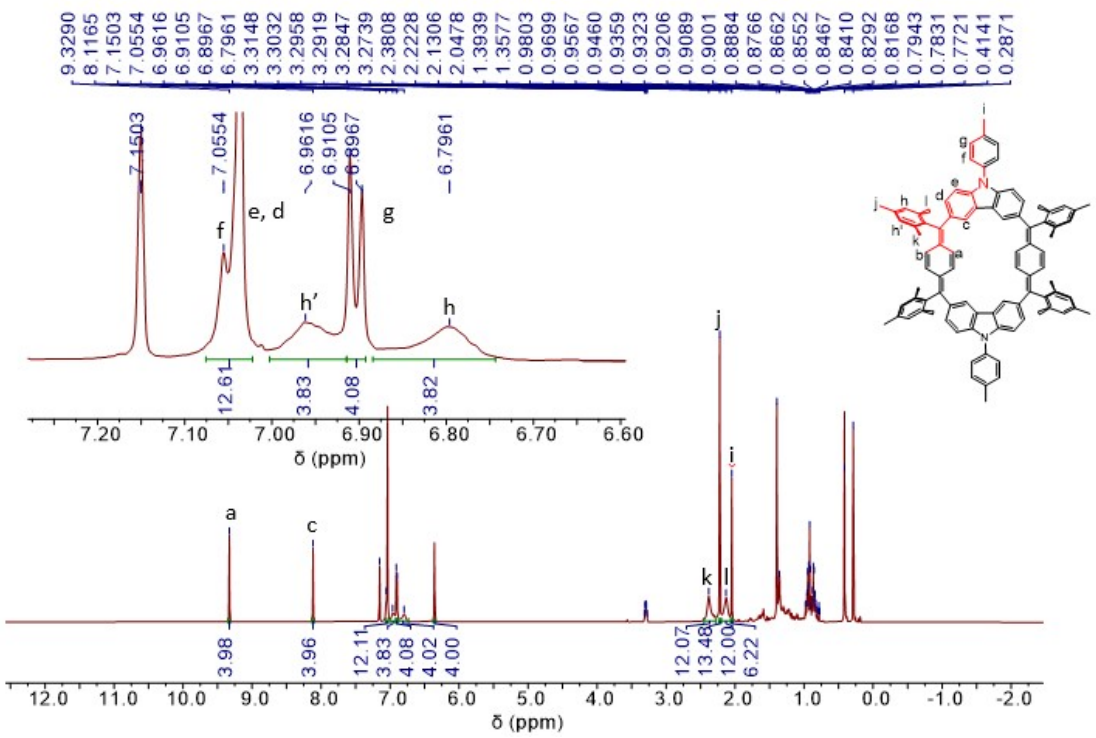

Figure S16. ^{1}H NMR (600 MHz) spectra of **CBQCz**. (600 MHz, C_6D_6, 25 °C).

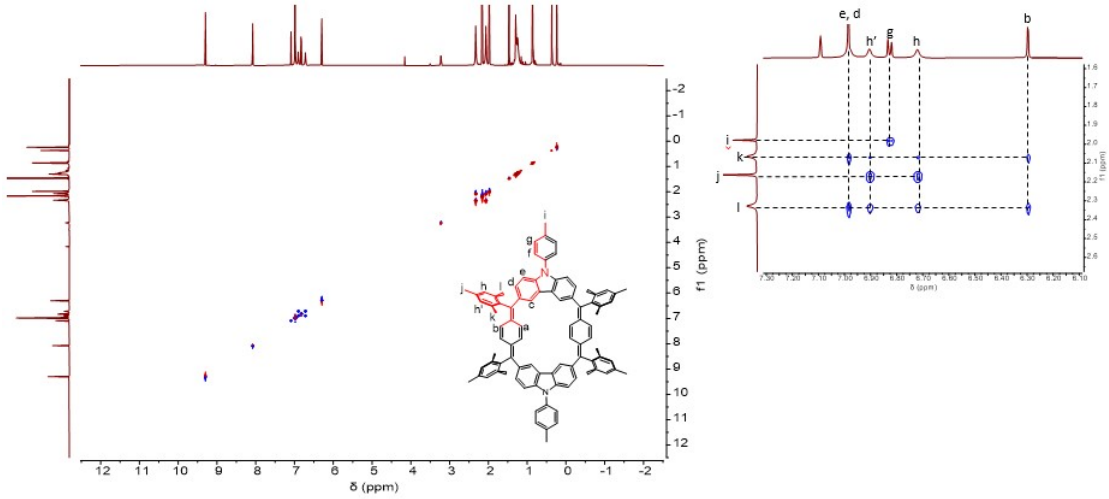

Figure S17. 2D ROESY NMR spectrum of **CBQCz** and partially zoomed spectrum with assignments (600MHz, C_6D_6, 7 °C).

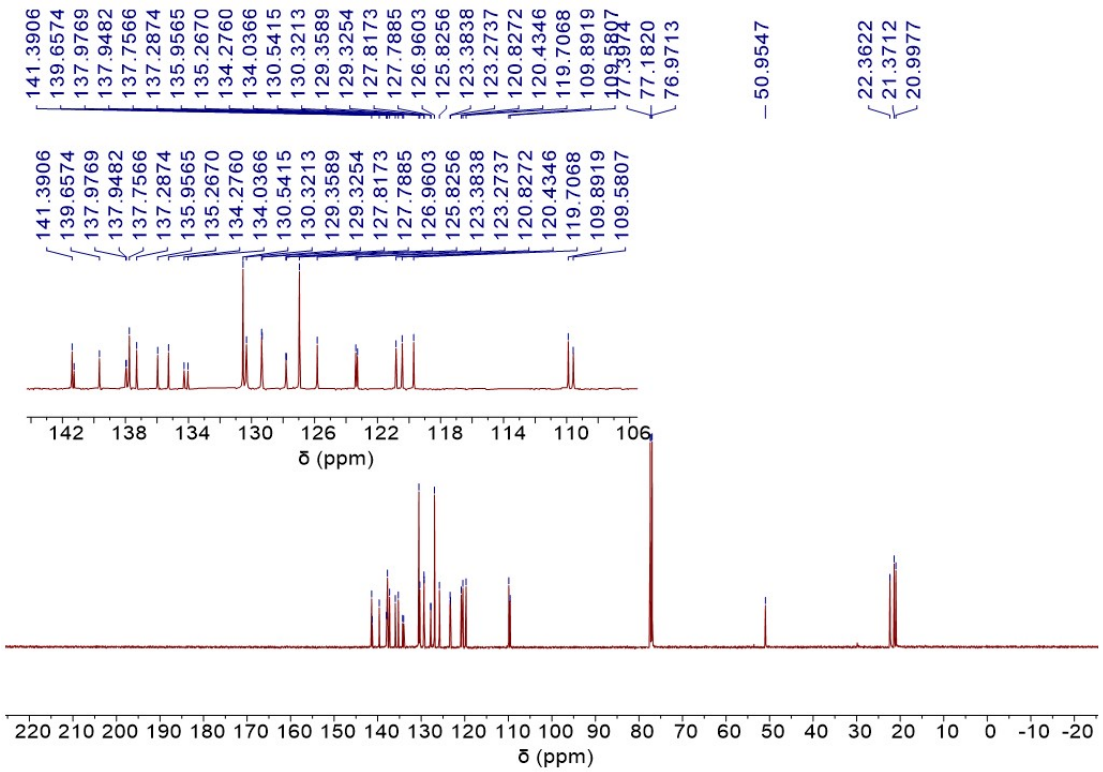

Figure S18. ^{13}C NMR spectrum of **CBQCz** (125 MHz, $CDCl_3$)

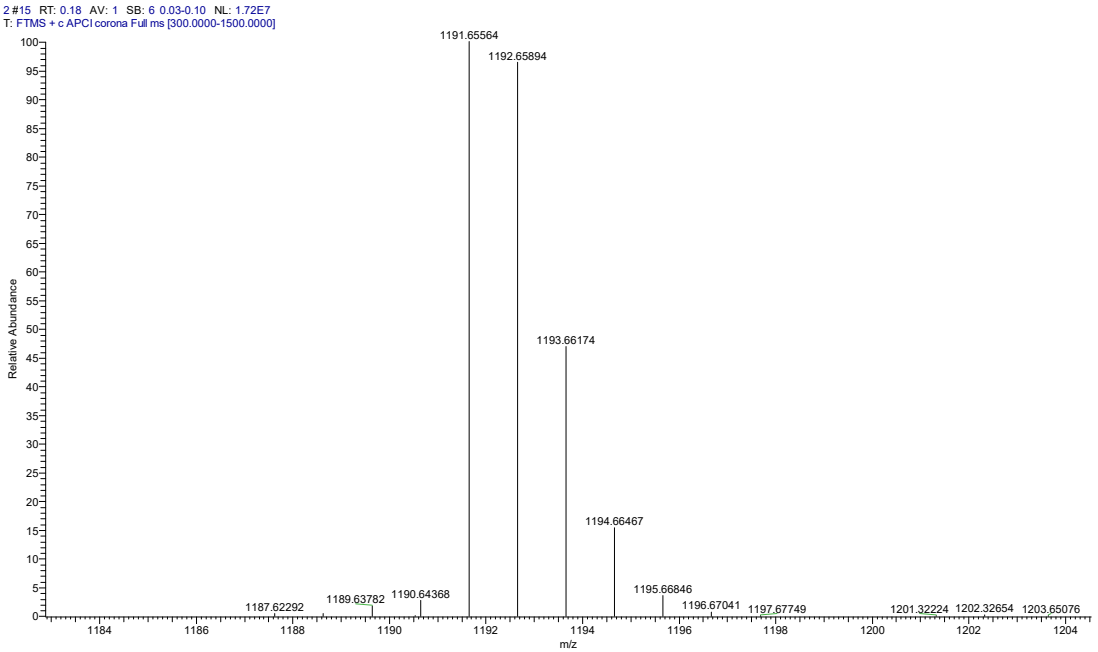

Figure S19. HR mass spectrum (APCI) of **3**.

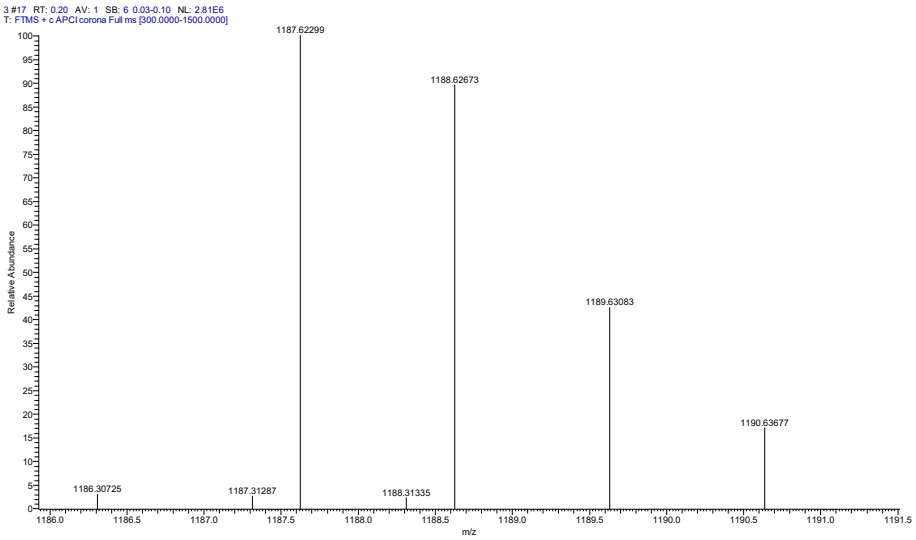

Figure S20. HR mass spectrum (APCI) of **CBQCz**.

9. References

1. M. Stępień, B. Szyszko, L. Latos-Grażyński, *Org. Lett*. **2009**, *11*, 3930.
2. H. Sharghi, S. Sepehri, M. Aberi, *Mol. Divers*., **2017**, *21*, 855-864.
3. (a) F. P. Gasparro, N. H. Kolodny, *J. Chem. Educ*., **1977**, *54*, 258; (b) J. Wang, X. Xu, H. Phan, T. S. Herng, T. Y. Gopalakrishna, G. Li, J. Ding, J. Wu, *Angew. Chem. Int. Ed*., **2017**, *56*, 14154-14158.
4. Gaussian 09; Revision A.2; Frisch, M. J.; Trucks, G. W.; Schlegel, H. B.; Scuseria, G. E.; Robb, M. A.; Cheeseman, J. R.; Scalmani, G.; Barone, V.; Mennucci, B.; Petersson, G. A.; Nakatsuji, H.; Caricato, M.; Li, X.; Hratchian, H. P.; Izmaylov, A. F.; Bloino, J.; Zheng, G.; Sonnenberg, J. L.; Hada, M.; Ehara, M.; Toyota, K.; Fukuda, R.; Hasegawa, J.; Ishida, M.; Nakajima, T.; Honda, Y.; Kitao, O.; Nakai, H.; Vreven, T.; Montgomery, J., J. A.; Peralta, J. E.; Ogliaro, F.; Bearpark, M.; Heyd, J. J.; Brothers, E.; Kudin, K. N.; Staroverov, V. N.; Kobayashi, R.; Normand, J.; Raghavachari, K.; Rendell, A.; Burant, J. C.; Iyengar, S. S.; Tomasi, J.; Cossi, M.; Rega, N.; Millam, N. J.; Klene, M.; Knox, J. E.; Cross, J. B.; Bakken, V.; Adamo, C.; Jaramillo, J.; Gomperts, R.; Stratmann, R. E.; Yazyev, O.; Austin, A. J.; Cammi, R.; Pomelli, C.; Ochterski, J. W.; Martin, R. L.; Morokuma, K.; Zakrzewski, V. G.; Voth, G. A.; Salvador, P.; Dannenberg, J. J.; Dapprich, S.; Daniels, A. D.; Farkas, Ö.; Foresman, J. B.; Ortiz, J. V.; Cioslowski, J.; Fox, D. J.; Gaussian, Inc., Wallingford CT, 2009.
5. A. D. Becke, *J. Chem. Phys*., 1993, 98, 5648.
6. C. Lee, W. Yang, R. G. Parr, Phys. Rev. *B: Condens. Matter.,* **1988**, *37*, 785.
7. R. Ditchfield, W. J. Hehre, J. A. Pople, *J. Chem. Phys*., **1971**, *54*, 724.
8. W. J. Hehre, R. Ditchfield, J. A. Pople, *J. Chem. Phys.*, **1972**, *56*, 2257.
9. P. C. Hariharan, J. A. Pople, *Theor. Chim. Acta*., **1973**, *28*, 213.
10. K. Yoneda, M. Nakano, Y. Inoue, T. Inui, K. Fukuda, Y. Shigeta, T. Kubo, B. Champagne, *J. Phys. Chem. C.*, **2012**, *116,* 17787-17795.